Mixing paints for generating metamerism art under 2 lights and 3 object colors

Daisuke Miyazaki, Kanami Takahashi, Masashi Baba,
Hirooki Aoki, Ryo Furukawa, Masahito Aoyama, Shinsaku Hiura,
Hiroshima City University
http://ime.info.hiroshima-cu.ac.jp/

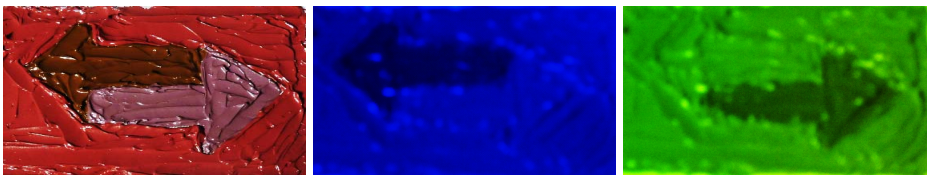

(a) (b) (c)

Figure 1. (a) Three kinds of mixed paints computed by the proposed method, (b) those illuminated by blue light, (c) those illuminated by yellow light.

Abstract

Metamerism is a phenomenon where two objects recognized as having different colors under one light are also recognized as having the same color under another light. This research proposes technology for actualizing artistic illusion that exploits metamerism. Specifically, the purpose of the research relates to automatic calculation of blending ratios of oil paints that cause metamerism to occur under specific light sources. We entails metamerism occurring between three types of object colors under two types of light sources. Also, we utilize plausible reflection model for the mixture of oil paints.

1. Introduction

The phenomenon where two objects recognized as having different colors under one light are also recognized as having the same color under another light is called metamerism. This research proposes technology for actualizing artistic illusion that exploits metamerism. Specifically, the purpose of the research relates to automatic calculation of paint blending ratios that cause metamerism to occur under specific light sources.

Metamerism, in which the colors of clothing and printed materials vary under fluorescent lighting and sunlight, is known as a source of annoyance among designers and photographers, and among those in the apparel, printing, and advertising industries. This paper rebels against such common sense, and fully brings out the value, disregarded in the past, of metamerism. Metamerism color charts are available commercially for confirming metamerism, but obtaining paints that cause metamerism under the user's desired light source is difficult for the average person. The development of automatic calculating software for the blending ratios of paints would allow production of metamerism works by even the average person in the apparel and advertising industries (without specialized knowledge in optics, such as spectra). In this paper, we show an artistic illusion, whose mixing ratio of oil paints are computed by our method, with three kinds of mixed paints (Fig. 1 (a)): Two of them becomes the same appearance under a certain colored light (Fig. 1 (b)), while another two paints becomes the same under different light (Fig. 1 (c)).

2. Related work

Works of media art have increased in number immensely over the past decades, in which digital technologies have been exploited in the creation of art. In particular, projection mapping onto large-scale architecture with the use of a projector has gained tremendous interest in the past few years. As the number of such media art works balloons, however, the problem arises that people grow accustomed to it. The same is true of analog artistic illusion: people get used to the existing artistic techniques, even though it can surprise people. Thus, the computer-assisted creation of analog artistic illusion has recently become the subject of research efforts to create new art that the human mind

would find difficult to accomplish. Hersch and Chosson [1] developed technology to represent premeditated pictures by exploiting Moiré patterns. Mitra and Pauly [2] developed technology for creating solids that generate premeditated shadow pictures when light is shone from three directions. Yue et al. [3] developed technology for designing transparent objects that enable expression of premeditated shapes by the concentration of light. Papas et al. [4] developed technology for designing transparent objects so that premeditated shapes can be represented when the objects are placed on an underlying illustration. These research fields are referred to as computer-assisted art illusions or computational art. The research of this paper considers metameric art like that produced by Valluzzi [5]. Although Valluzzi [5] had no goal of representing any premeditated shapes, the purpose of this research is the blending of paints to generate metamerism to thus enable the representation of premeditated shapes.

Research into metamerism has existed for a long time, but little research has exploited metamerism for art. Bala et al. [6] engaged in research to create watermarks using metamerism. For a CMYK printer, the printing of black is represented as the "K" (key) ink or the "CMY" (cyan, magenta, yellow) inks. Hence, calculations were made for the representation of a black object color by using as much K ink as possible and as little CMY ink as possible, and by using as much CMY ink as possible and as little K ink as possible for an object's color. These are observed as the same color under natural light, but as different colors when exposed to LEDs of specific wavelengths. Two types of LEDs were prepared, and the largest difference in their wavelengths was based on comparison of their spectral distributions. Contrary to the research of Bala et al. [6], our research blended paints that generated the most metamerism under light sources designated by the user. To also represent spectral distributions that four colors of ink cannot, the optimum combination of paints was selected from among many more types.

Drew and Bala [7] took the two types of object colors prepared by Bala et al. [6], photographed them with an ordinary camera, and converted the colors by multiplying 3×3 matrix for emphasizing metamerism. Using virtual LEDs of 31 colors, they also proposed a method for searching for combinations that generated the greatest metamerism among all combinations attainable by individually turning on and off each LED. Because the spectral distributions of the virtual LEDs did not actually exist, the paper of Drew and Bala [7] described no experiment on actual objects. Since the purpose of our paper is to be observed by the human eye, the colors after observation cannot be converted by the 3×3 matrix for emphasizing metamerism. Instead, we propose a method for calculating blending ratios of paints that produce the most emphasis in metamerism. Our experiment also demonstrates in real world by employing the spectral distributions of actually existing light sources.

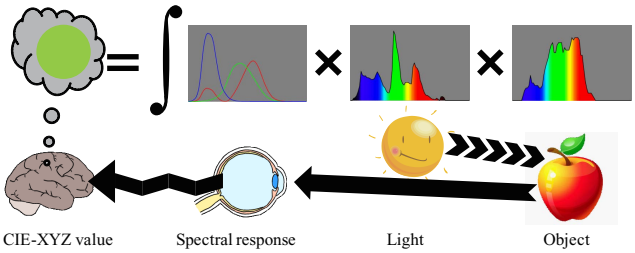

Figure 2. Principle of perceiving visible light.

Miyazaki et al. [8] proposed a method for calculating the blending ratios of paint that generate the greatest metamerism in response to light sources designated by the user. Miyazaki et al. worked on metamerism occurring between two types of object colors under two types of light sources, but our research entails metamerism occurring between three types of object colors under two types of light sources. Moreover, they represented object colors by an additive color mixture, but our research employs the reflection model suited to represent object colors.

Finlayson et al. [9, 10] proposed a method for calculating spectral distributions that generate metamerism, as well as a method for estimating many spectral distributions observed as the same color as given RGB values or XYZ values. Spectral distributions observed as the same color exist infinitely in theory; however, the variation of paints that cause metamerism is limited in reality. Therefore, they limit the metamer sets to be a linear sums of the spectral distributions of each patch of Macbeth ColorChecker, manufactured by X-Rite, Inc. As the purpose of our research is to reproduce with real paints, the spectral distributions of oil paints were used from a database rather than from the Macbeth ColorChecker. Unlike light, object colors are represented under a subtractive color mixture rather than linear sums of spectral distributions. Thus, we calculate object colors using a reflection model suited for object colors.

Morimoto et al. [11] described the importance of metamerism and noted that spectral distribution analysis was indispensable for the digital archiving cultural assets. Johnson and Fairchild [12] also described the importance of metamerism and showed the need to calculate colors from spectral distributions rather than from RGB values for computer graphics generation. Our research demonstrates the usefulness of metamerism by its use in art.

3. Principles of reflection

A typical method of expressing human perception of color concerns the XYZ color system defined by the International Commission on Illumination (CIE). The system

can represent the color sensed by the brain, based on stimuli obtained from photoreceptor cells. X, Y, and Z, correspond to recognition of red, green, and blue colors, respectively. This research utilizes the wavelength data of light from 400 to 800 nm. Suppose that the color matching functions of X, Y, and Z are $\bar{x}(\lambda)$, $\bar{y}(\lambda)$, and $\bar{z}(\lambda)$, respectively, as a function of wavelength λ, the observed value X, Y, and Z of the scene can be represented as follows (Fig. 2).

$$X = \int_{400}^{800} E(\lambda)S(\lambda)\bar{x}(\lambda)d\lambda\,, \tag{1}$$

$$Y = \int_{400}^{800} E(\lambda)S(\lambda)\bar{y}(\lambda)d\lambda\,, \tag{2}$$

$$Z = \int_{400}^{800} E(\lambda)S(\lambda)\bar{z}(\lambda)d\lambda\,, \tag{3}$$

where $E(\lambda)$ represents the spectral distribution of the light source and $S(\lambda)$ represents the spectral reflectance of the object surface. Above equations suppose that spectral distribution is calculated as a continous function; however, we cannot measure the spectral distribution as a continous function but can measure them as a discretized value. In our research, we suppose that the spectral distribution are represented as N_b number of values, where the wavelength data of visible light from 400 to 800 nm are discretized with equal intervals. Denoting $\mathbf{x} = (X, Y, Z)^\top$ as the observed value, Eq. (1), Eq. (2), and Eq. (3) are represented as following equation.

$$\mathbf{x} = \mathbf{PEs}\,. \tag{4}$$

Here, discrete data of the color matching functions are represented by the $3 \times N_b$ matrix $\mathbf{P}$, of which the first to third rows are color matching functions of X, Y, and Z.

$$\mathbf{P} = \begin{pmatrix} \bar{x}_1 & \cdots & \bar{x}_{N_b} \\ \bar{y}_1 & \cdots & \bar{y}_{N_b} \\ \bar{z}_1 & \cdots & \bar{z}_{N_b} \end{pmatrix}. \tag{5}$$

The spectral reflectance of the object surface is represented as the $N_b \times 1$ vector $\mathbf{s}$. $N_b \times N_b$ diagonal matrix $\mathbf{E}$ represents the spectral distributions of light source.

$$\mathbf{E} = \mathrm{diag}\,(E_1, E_2, \cdots, E_{N_b})\,. \tag{6}$$

4. Proposed method

This section describes the method for automatic calculation of oil paint blending ratios that cause metamerism to occur. Two different light sources are labeled as Light Source 1 and Light Source 2. Three different types of paint mixed from multiple oil paints are labeled Mixed Paint 1, Mixed Paint 2, and Mixed Paint 3. The purpose of this research is to reproduce the following phenomena: Under Light Source 1, Mixed Paint 1 and Mixed Paint 3 appear as the same color and brightness, while Mixed Paint 2 and Mixed Paint 3 appear as different colors and brightness values; under Light Source 2, Mixed Paint 2 and Mixed Paint 3 appear as the same color and brightness, while Mixed Paint 1 and Mixed Paint 3 appear as different colors and brightness values (Fig. 3).

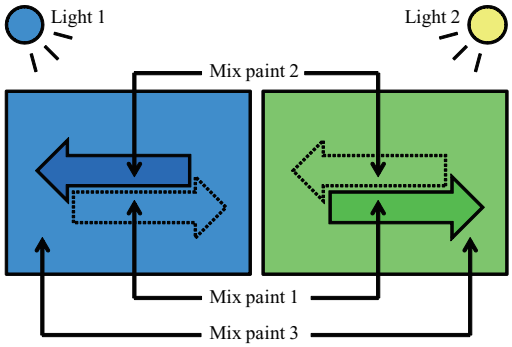

Figure 3. Metamerism of three sets of mixed paint illuminated by two different lights.

The database of spectral reflectance for N_p types of paint necessary for mixing the paints is represented as the $N_b \times N_p$ matrix $\mathbf{D}$.

$$\mathbf{D} = \begin{pmatrix} d_{11} & d_{12} & \cdots & d_{1N_p} \\ d_{21} & d_{22} & \cdots & d_{2N_p} \\ \vdots & \vdots & \ddots & \vdots \\ d_{N_b1} & d_{N_b2} & \cdots & d_{N_bN_p} \end{pmatrix}. \tag{7}$$

Mixed paint is prepared by combining the N_p paints with N_p mixing proportions. The mix ratios are represented as the $N_p \times 1$ vector $\mathbf{w}$.

Assuming the paint mixing to be additive color mixing, Miyazaki et al. [8] calculated the spectral reflectances of mixed paint. But real paint is subject to subtractive paint mixing; therefore, a reflection model suited to the paint must be used.

The model by Curtis et al. [13] exists for water-color paint, but for this type of paint, the base color and water content cause the observed color to differ from when it was blended. The model is therefore not suited for this research.

Tominaga and Nishi [14] measured the spectral reflectance of oil paint. After measuring actual oil paint, Tominaga and Nishi [14] concluded that the diffuse reflection components of oil paint depended neither on applied thickness nor the amount of solvent oil. The Kubelka-Munk theory is a method for representing multi-layer reflection; however, the Kubelka-Munk model is not suited to oil paint, based on findings by Tominaga and Nishi [14] of the non-dependence on applied thickness. No dependence on applied thickness means that transparency is low; therefore, models of sub-surface scattering such as the dipole model are also not suited for oil paint. Therefore, oil paint can be

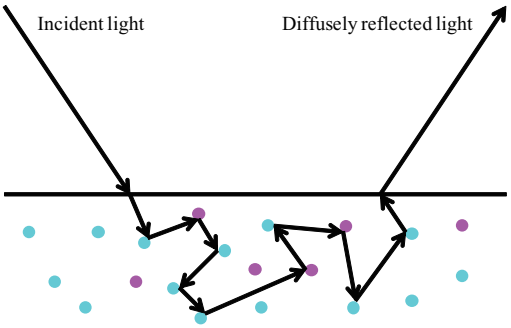

Figure 4. Diffuse reflection of mixed paint.

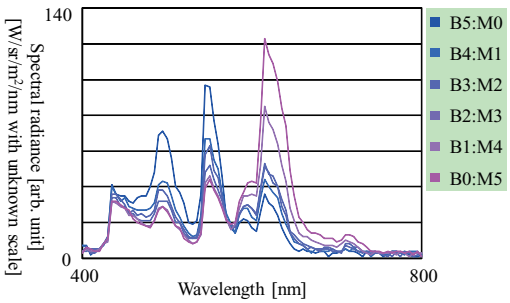

Figure 5. Difference of spectral distribution with different mixing ratio of two paints, HORIZON BLUE and LIGHT MAGENTA, illuminated by artificial sunlight.

represented with the Lambert reflection model. Tominaga et al. [15] estimated the surface normals of picture art with the photometric stereo method, exploiting the fact that diffuse reflection components of oil paint could be represented by the Lambert reflection model.

Based on the findings of Tominaga and Nishi [14], our research also employed the Lambert reflection model as the model for diffuse reflection components of oil paint. Specular reflection components are not considered in this paper, since they are unrelated to our purpose. Because ideal diffuse reflection is assumed, light incident to the inside of the object randomly reflects off internal particles a sufficient number of times before exiting. Because it is an ideal diffuse reflection, no effect is sustained from particle size or particle density. In such a case, the spectral reflectance of mixed paint can be calculated with the following equation.

$$\mathbf{s} = \mathbf{D}^{\mathbf{w}} \equiv \begin{pmatrix} d_{11}^{w_1} \times d_{12}^{w_2} \times \cdots \times d_{1N_p}^{w_{N_p}} \\ d_{21}^{w_1} \times d_{22}^{w_2} \times \cdots \times d_{2N_p}^{w_{N_p}} \\ \vdots \\ d_{N_b1}^{w_1} \times d_{N_b2}^{w_2} \times \cdots \times d_{N_bN_p}^{w_{N_p}} \end{pmatrix}. \quad (8)$$

This model is known as the transmission model. The same phenomenon occurs for transmitted light and diffusely reflected light: Light penetrating a substance is reflected and absorbed by internal particles and then exits.

Now, we introduce a specific example to explain the physical meaning of the reflection model shown as Eq. (8). The mixed paint obtained from combination of 70% paint with reflectance $d_1(\lambda)$ and 30% paint with reflectance $d_2(\lambda)$ has reflectance of $d_1(\lambda)^{7/10} d_2(\lambda)^{3/10}$, which is evident from Fig. 4. This is because, as this is an ideal diffuse reflection, the internal particles are reflected off a sufficient number of times inside the object, meaning the particle reflections occur under the same probability as the blend ratio.

To determine whether this reflection model was appropriate in practice, spectral distributions were analyzed for mixes of actual oil paints. Spectra data for pigment mixes of Horizon Blue (B) and Light Magenta (M) in six stages in

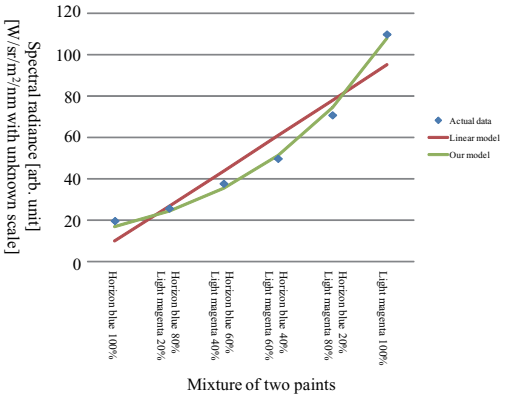

Figure 6. Intensity plot with different mixture ratio of two paints ($\lambda = 625$nm).

proportions of $5:0$, $4:1$, $3:2$, $2:3$, $1:4$, and $0:5$ were taken, as shown in Fig. 5. Data for the wavelength of 625 nm were extracted from Fig. 5 and provided in Fig. 6. In Fig. 6, the vertical axis represents the photographed spectral radiance and the horizontal axis represents the mix ratios of Horizon Blue and Light Magenta. The straight line drawn in Fig. 6 provides radiance calculations for additive color mixing [8, 9, 10], and the curve drawn in Fig. 6 provides the radiance calculated with the model of Eq. (8). Because paints embody subtractive color mixing, there is a trend of being darker than the radiance predicted under additive color mixing. Eq. (8) is suited for the representation of reflection for paints, and is therefore used in this research.

As a result, the cost function $F(\cdot)$ to be minimized in

order to fulfil our purpose (Fig. 3) is as follows.

$$
\begin{aligned}
&F(\mathbf{P},\mathbf{E}_1,\mathbf{E}_2,\mathbf{D},\mathbf{w}_1,\mathbf{w}_2,\mathbf{w}_3) = \\
&\|\mathbf{P}\mathbf{E}_1\mathbf{D}^{\mathbf{w}_1} - \mathbf{P}\mathbf{E}_1\mathbf{D}^{\mathbf{w}_3}\|^2 \\
&+ \|\mathbf{P}\mathbf{E}_2\mathbf{D}^{\mathbf{w}_2} - \mathbf{P}\mathbf{E}_2\mathbf{D}^{\mathbf{w}_3}\|^2 \\
&- \|\mathbf{P}\mathbf{E}_1\mathbf{D}^{\mathbf{w}_2} - \mathbf{P}\mathbf{E}_1\mathbf{D}^{\mathbf{w}_3}\|^{0.5} \\
&- \|\mathbf{P}\mathbf{E}_2\mathbf{D}^{\mathbf{w}_1} - \mathbf{P}\mathbf{E}_2\mathbf{D}^{\mathbf{w}_3}\|^{0.5}, \qquad (9)
\end{aligned}
$$

$$
\begin{aligned}
&\{\mathbf{w}_1,\mathbf{w}_2,\mathbf{w}_3\} = \\
&\underset{\mathbf{w}_1,\mathbf{w}_2,\mathbf{w}_3}{\operatorname{argmin}} F(\mathbf{P},\mathbf{E}_1,\mathbf{E}_2,\mathbf{D},\mathbf{w}_1,\mathbf{w}_2,\mathbf{w}_3), \qquad (10)
\end{aligned}
$$

$$
\begin{aligned}
&\text{s.t.} \quad \sum_{n=1}^{N_p} w_{1n} = 1,\ \sum_{n=1}^{N_p} w_{2n} = 1,\ \sum_{n=1}^{N_p} w_{3n} = 1, \\
&\quad 0 \le w_{1n},\ 0 \le w_{2n},\ 0 \le w_{3n}, \quad \{n = 1,\cdots,N_p\}.
\end{aligned}
$$

Since Eq. (10) is a complicated function with constraint conditions, simulated annealing based on the Nelder-Mead downhill simplex method [16] was adopted to solve the equation stably. The Nelder-Mead downhill simplex method is not the simplex method of linear programming, but a type of algorithm that minimizes the cost function. The cost function in Eq. (9) is not in quadratic form and may even take negative values. Thus, neither Newton's method nor the Levenberg-Marquardt method can be applied. The solution therefore requires the steepest descent method, the conjugate gradient method, the genetic algorithm, or the Nelder-Mead downhill simplex method. The convergency speed of the genetic algorithm is slow. The steepest descent method and conjugate gradient method require C^1 (first-order differentiable) smoothness for the cost function, but the Nelder-Mead downhill simplex method does not require the function to be differentiable. Eq. (9) is a smooth function, but the spectral distribution of the database is not a smooth distribution. Thus, the Nelder-Mead downhill simplex method was used as a precaution. The Nelder-Mead downhill simplex method derives solutions in a stable manner and thus is commonly used [17]. This algorithm was thus used for our research. Eq. (9) is not unimodal and can be problematic in readily tending to a local solution. To avoid falling into a local solution, simulated annealing was used. Since certain papers note that simulated annealing is effective in the problem of estimating parameters of some kind by exploiting multi-spectral data [18, 19], this research also adopted this algorithm. The source code of Press et al. [16] was utilized for implementation of the algorithm combining the Nelder-Mead downhill simplex method and simulated annealing.

Eq. (9) employs addition and subtraction; however, multiplication and division may be used instead. A preliminary experiment confirmed that similar results could be obtained in either case. However, the calculations become unstable as the denominator approaches zero when multiplication and division are used. The preliminary experiment could not confirm this phenomenon and stability could be provided with the addition of a positive constant to the denominator; nevertheless, this research opted to use Eq. (9) as a precaution. Note that multiplication and division becomes addition and subtraction if we calculate logarithm; therefore, there is only a small difference between the cost function that uses multiplication and division and that uses addition and subtraction.

The first and second terms of Eq. (9) were squared to increase their weighting, and the third and fourth terms were taken to the 0.5 power to decrease their weighting. Since human vision recognizes subtle changes in color or brightness with emphasis, weighting of the first and second terms that make color and brightness the same was increased, while weighting of the third and fourth terms that make color and brightness different was decreased. Another reason for this treatment relates to the difficulty in discovering spectral distributions that produce the same color and the infinite existence of spectral distributions that produce different colors. The preliminary experiment empirically confirmed that Eq. (9) could more stably determine a solution, even more so than the case where all terms were squared.

5. Experimental results

A hyper-spectral camera HSC-1700 (Fig. 7) was used to photograph the spectral data from 400 nm to 800 nm. Radiance could be analyzed for a total of 81 bands ($N_b = 81$) from 400 nm to 800 nm in 5 nm intervals. Spectral distributions were analyzed for 29 types ($N_p = 29$) of different color oil paints (Fig. 9), which were exposed to an artificial sunlight. Since brightness as well as chromaticity influence the result, the paint database of 29 types included white and black paints for adjusting brightness. The artificial sunlight (Fig. 10) is the Probright V manufactured by Nippon Paint Co., Ltd. with a color temperature of 6500 K and color rendering performance of Ra98. The 29 spectral distributions were divided by the spectral distribution of a white perfect diffuser (Fig. 8) exposed to the artificial sunlight in order to yield spectral reflectances utilized as database $\mathbf{D}$. The spectral distributions of all 29 types of oil paints are shown in Fig. 11 and represent the distributions exposed to the artificial sunlight. Subsequent processing utilized spectral reflectances that were derived by division of the above by the spectral distribution of the white diffuser.

The mixing proportions were initially calculated for 29 colors ($N_p = 29$) and recalculated for 10 colors of paint ($N_p = 10$) with blending ratios exceeding the threshold value. The reason for this procedure is the fact that, in reality, the operation of mixing paints becomes complicated as the number of paints to be blended grows large, and not because of any problem arising from the proposed algorithms. Based on the blending ratios determined, actual paints were mixed and visually confirmed to deliver the results envi-

Figure 7. Hyper-spectral camera HSC-1700 manufactured by Eba Japan Co., Ltd.

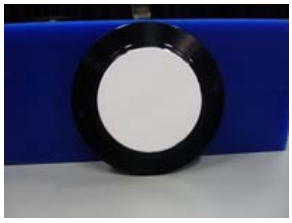

Figure 8. Diffuse white reflectance standard.

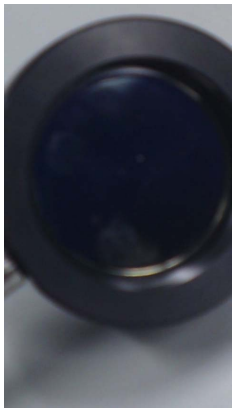

Figure 12. Blue narrow band filter (peak = 460 nm, bandwidth = 10 nm).

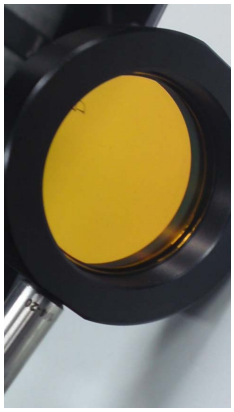

Figure 13. Yellow narrow band filter (peak = 577 nm, bandwidth = 10 nm).

Figure 9. 29 types of oil paints included in the database.

Figure 10. Artificial sunlight Probright V manufactured by Nippon Paint Co., Ltd.

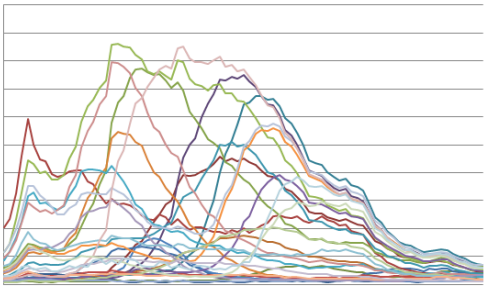

Figure 11. Whole 29 spectral distributions of oil paintings used as database. These spectral distributions represent the observed intensity, and do not represent spectral reflectances; namely, the spectral distribution of those are not divided by the spectral distribution of the artificial sunlight.

sioned in Fig. 3, and the results are shown in Fig. 1. Moreover, paint was not applied in layers, but after stirring, so that all paint colors were completely mixed and applied in such a way that the base was not visible. Interference filters shown in Fig. 12 and Fig. 13 were utilized to provide light sources of two colors. Since the artificial sunlight was large, the filters were not installed in front of the light source, but in front of the camera for photographs. The same light can be observed whether the filter is installed in front of the light source or in front of the camera, because the subject is an ideal Lambert object that generates no change to wavelengths, such as interference or dispersion.

Calculations were made for each paint type and not on a pixel-unit basis. In this case, calculations were made for three types of mixed paints. The calculation time for operating the single-core Intel Xeon 2.50 GHz CPU was 19.16 seconds when utilizing the 29-color database.

6. Discussion

The solution depends on the oil paint database. If the spectral distributions of the database form 81 orthonormal bases, then any spectral distribution can be represented, and thus, a solution necessarily exists (except for ill-posed setting issues, such as identical spectral distributions for the two light sources). Spectral distributions of actual oil paints, however, are not exclusively linearly independent. Paint is formed from pigment (particles) originated from minerals. This means that the types of pigments used in actual paints are finite.

Hence, the principal components were analyzed for all 29 types of paints in the database. The spectral distributions obtained from the database are shown in Fig. 11. The top nine eigenvalues along with the contribution ratios and cumulative contribution ratios obtained as a result of the prin-

Table 1. Cumulative proportion of variance from the first eigenvalue to the nineth eigenvalue.

	Eigenvalue	Variance (%)	Cumulative (%)
1	46.17	57.00	57.00
2	22.36	27.60	84.60
3	8.34	10.30	94.90
4	2.43	3.00	97.89
5	0.71	0.87	98.77
6	0.53	0.66	99.43
7	0.24	0.29	99.72
8	0.13	0.15	99.87
9	0.04	0.05	99.92

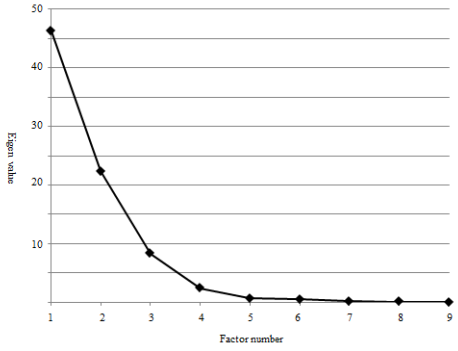

Figure 14. Scree plot of the top nine PCs.

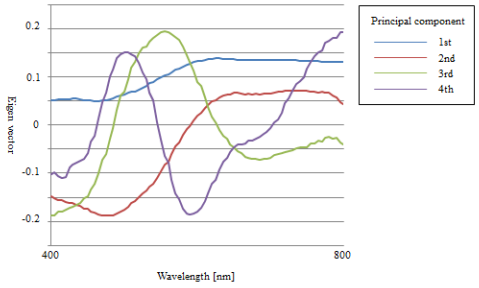

Figure 15. PCs of the largest four eigenvalues.

cipal component analysis are shown in Table 1. The top nine eigenvalues are plotted in Fig. 14, and the eigenvectors of the top four principal components are graphed in Fig. 15. According to Table 1, the cumulative contribution ratios exceed 95% with the fourth eigenvalue, 99% with the sixth eigenvalue, and 99.9% with the ninth eigenvalue. These results mean that even with a database of 29 types of paint, the amount of information contained is comparable to just 4 to 9 types.

Parkkinnen et al. [20] analyzed spectral distributions of various kinds of objects and showed that all object colors within the database could be completely represented by the top eight basis functions. Judd et al. [21], Cohen [23], Maloney [24], and Vrhel et al. [25] have performed similar analyses and reached similar conclusions. Especially, the similar conclusion for oil paints' database is derived by Tominaga and Tanaka [22]. Our experiment confirmed that the affirmations of these papers are also valid for our choice of oil paints.

The experiment showed that representing arbitrary spectral distributions was impossible with actual paint. The proposed method involves calculating with simulated annealing so that metamerism is generated as much as possible, but the desired solution may not necessarily be obtained, depending on the conditions and light source colors used for generating metamerism and the paint database. However, the results also showed that metamerism could be generated with just 4 to 9 types of paint. The actual experiment did not directly use blending ratios of all 29 types of paint. Instead, 10 of them with the largest percentages were selected, and the paints were mixed after the blending proportions had been determined again with the selected paints.

7. Conclusion

This research confirmed the occurrence of metamerism between three object colors and two light sources. The purpose was to generate metamerism under a light source designated by the user. Methods to automatically select or blend light sources from a light source database to generate optimum metamerism are planned for future work.

Morovič et al. [26] argued that printers that use 11 colors of ink are useful for printing spectral distributions of various object colors. Tzeng and Berns [27] also conducted research on printers that use four or six colors of ink. A future task is to join with printer manufacturers to develop printers capable of printing spectral distributions of various object colors.

In this research and the research of Miyazaki et al. [8], metamerism was emphasized with the blending of paints. Drew and Bala [7] emphasized metamerism with combinations of LED light sources. For the future, the automatic selection of optimum light source combinations is being considered, rather than the blending of paints only, to generate stronger metamerism than in this and other existing research [8, 7].

As a course of action for the future, a database with the spectral distributions of oil paints and the spectral distributions of widely commercially available lighting and software on the Internet are being considered, so that general users who have no instruments for measuring spectral distribution can produce works of metamerism art with Holbein commercial oil paints.

Acknowledgments

This research was supported in part by the Grant-in-Aid for Scientific Research on Innovative Areas "Shitsukan" (no. 22135003) from MEXT, Japan, and in part by the Grant-in-Aid for Young Scientists (no. 24700176) from JSPS, Japan. The authors thank Naoki Asada for useful discussions. They also thank anonymous reviewers for their careful reviews of the paper.

References

[1] R. D. Hersch and S. Chosson, "Band moiré images," SIGGRAPH 2004 Papers, pp. 239–247, 2004. 2

[2] N. J. Mitra and M. Pauly, "Shadow art," ACM Trans. Graph., vol. 28, no. 5, article 156, 7 pages, 2009. 2

[3] Y. Yue, K. Iwasaki, B. Chen, Y. Dobashi, and T. Nishita, "Pixel art with refracted light by rearrangeable sticks," Computer Graphics Forum, vol. 31, no. 2, pp. 575–582, 2012. 2

[4] M. Papas, T. Houit, D. Nowrouzezahrai, M. Gross, and W. Jarosz, "The magic lens: refractive steganography," ACM Trans. Graph., vol. 31, no. 6, article 186, 10 pages, 2012. 2

[5] R. Valluzzi, "LEDs illuminat metamerism in abstract art - no 2," `http://www.youtube.com/watch?v=fyJHlinM730`, 2012. 2

[6] R. Bala, K. M. Braun, and R. P. Loce, "Watermark encoding and detection using narrowband illumination," in Proceedings of Seventeenth Color Imaging Conference, pp. 139–142, 2009. 2

[7] M. S. Drew and R. Bala, "Sensor transforms to improve metamerism-based watermarking," in Proceedings of 18th Color Imaging Conference, pp. 22–26, 2010. 2, 7

[8] D. Miyazaki, K. Nakamura, M. Baba, R. Furukawa, M. Aoyama, S. Hiura, and N. Asada, "A first introduction to metamerism art," SIGGRAPH ASIA Posters, 2012. 2, 3, 4, 7

[9] A. Alsam and G. Finlayson, "Metamer sets without spectral calibration," J. Opt. Soc. Am. A, vol. 24, no. 9, pp. 2505–2512, 2007. 2, 4

[10] G. D. Finlayson and P. Morovic, "Metamer sets," J. Opt. Soc. Am. A, vol. 22, no. 5, pp. 810–189, 2005. 2, 4

[11] T. Morimoto, T. Mihashi, and K. Ikeuchi, "Color restoration method based on spectral information using normalized cut," International Journal of Automation and Computing, vol. 5, no. 3, pp. 226–233, 2008. 2

[12] G. Johnson and M. Fairchild, "Full-spectral color calculations in realistic image synthesis," IEEE Computer Graphics and Applications, vol. 19, no. 4, pp. 47–53, 1999. 2

[13] C. J. Curtis, S. E. Anderson, J. E. Seims, K. W. Fleischer, and D. H. Salesin, "Computer-generated watercolor," in Proceedings of the 24th annual conference on Computer graphics and interactive techniques (SIGGRAPH '97), pp. 421–430, 1997. 3

[14] S. Tominaga and S. Nishi, "Surface reflection properties of oil paints under various conditions," Proc. SPIE 6807, 2008. 3, 4

[15] S. Tominaga, H. Ujike, and T. Horiuchi, "Surface reconstruction of oil paintings for digital archiving," Proc. IEEE Southwest Symposium on Image Analysis & Interpretation, pp. 173–176, 2010. 4

[16] W. H. Press et al., "Numerical recipes in C: the art of scientific computing," Cambridge: Cambride University Press, 994 p., 1997. 5

[17] J. Takamatsu, Y. Matsushita, and K. Ikeuchi, "Estimating camera response functions using probabilistic intensity similarity," in Proceedings on IEEE Conference on Computer Vision and Pattern Recognition, 8 p., 2008. 5

[18] A. Ikari, R. Kawakami, R. T. Tan, and K. Ikeuchi, "Separating illumination and surface spectral from multiple color signals." In *Digitally archiving cultural objects* (pp. 297–321), Springer US, 2008. 5

[19] P.-R. Chang and T.-H. Hsieh, "Constrained non-linear optimization approaches to color-signal separation," IEEE Trans. Image Processing, vol. 4, no. 1, pp. 81–93, 1995. 5

[20] J. P. S. Parkkinen, J. Hallikainen, and T. Jaaskelainen, "Characteristic spectra of Munsell colors," J. Opt. Soc. Am. A, vol. 6, no. 2, pp. 318–322, 1989. 7

[21] D. B. Judd, D. L. MacAdam, and G. W. Wyszecki, "Spectral distribution of typical daylight as a function of correlated color temperature," J. Opt. Soc. Am., vol. 54, pp. 1031–1040, 1964. 7

[22] S. Tominaga and N. Tanaka, "Spectral image acquisition, analysis, and rendering for art paintings," Journal of Electronic Imaging, vol. 17, no. 4, pp. 043022-043022-13, 2008. 7

[23] J. Cohen, "Dependency of the spectral reflectance curves of the Munsell color chips," Psychonomical Science, vol. 1, pp. 369–370, 1964. 7

[24] L. T. Maloney, "Evaluation of linear models of surface spectral reflectance with small numbers of parameters," J. Opt. Soc. Am. A, vol. 10, pp. 1673–1683, 1986. 7

[25] M. J. Vrhel, R. Gershon, and L. S. Iwan, "Measurement and analysis of object reflectance spectral," Color Res. and Appl., vol. 19, pp. 4–9, 1994. 7

[26] P. Morovič, J. Morovič, J. Arnabat, and J. M. García-Reyero, "Revisting spectral printing: a data driven approach," in Proceedings of 20th Color Imaging Conference, pp. 335–340, 2012. 7

[27] D.-Y. Tzeng and R. S. Berns, “Spectral-based six-color separation minimizing metamerism,” in Proceedings of IS&T/SID Eighth Color Imaging Conference, pp. 342–347, 2000. 7